Sustainable Cities and Society 99 (2023) 104872

Contents lists available at ScienceDirect

Sustainable Cities and Society

journal homepage: www.elsevier.com/locate/scs

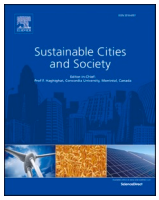

Combined and delayed impacts of epidemics and extreme weather on urban mobility recovery

Haiyan Liu [a,*,#], Jianghao Wang [b,c,#], Jian Liu [a], Yong Ge [b,c], Xiaoli Wang [d], Chi Zhang [e], Eimear Cleary [f], Nick W. Ruktanonchai [g], Corrine W. Ruktanonchai [g], Yongcheng Yao [f,h], Amy Wesolowski [i], Xin Lu [j,m], Andrew J. Tatem [f], Xuemei Bai [k,*], Shengjie Lai [f,l,m,*]

[a] Ocean Data Center, Southern Marine Science and Engineering Guangdong Laboratory (Zhuhai), Zhuhai, Guangdong 528478, China
[b] State Key Laboratory of Resources and Environmental Information System, Institute of Geographic Sciences and Natural Resources Research, Chinese Academy of Sciences, Beijing 100101, China
[c] University of Chinese Academy of Sciences, Beijing 100101, China
[d] Beijing Center for Disease Prevention and Control, Beijing 100021, China
[e] School of Public Health (Shenzhen), Sun Yat-sen University, Shenzhen, Guangdong 528406, China
[f] WorldPop, School of Geography and Environmental Science, University of Southampton, Southampton SO17 1BJ, UK
[g] Population Health Sciences, Virginia Tech, Blacksburg, VA 24060, USA
[h] Zhengzhou Normal University, Zhengzhou, Henan 450044, China
[i] Department of Epidemiology, Johns Hopkins Bloomberg School of Public Health, Baltimore, MD 21218, USA
[j] College of Systems Engineering, National University of Defense Technology, Changsha, Hunan 410073, China
[k] Fenner School of Environment and Society, Australia National University, Canberra, ACT 2600, Australia
[l] Institute for Life Sciences, University of Southampton, Southampton SO17 1BJ, UK
[m] Shanghai Institute of Infectious Disease and Biosecurity, Fudan University, Shanghai 200433, China

ARTICLE INFO

Keywords:
Compound disasters
Mobility recovery
Epidemic
Extreme weather
Nonlinear delayed effects
Urban resilience

ABSTRACT

The ever-increasing pandemic and natural disasters might spatial-temporal overlap to trigger compound disasters that disrupt urban life, including human movements. In this study, we proposed a framework for data-driven analyses on mobility resilience to uncover the compound effects of COVID-19 and extreme weather events on mobility recovery across cities with varied socioeconomic contexts. The concept of suppression risk (SR) is introduced to quantify the relative risk of mobility being reduced below the pre-pandemic baseline when certain variables deviate from their normal values. By analysing daily mobility data within and between 313 Chinese cities, we consistently observed that the highest SR under outbreaks occurred at high temperatures and abnormal precipitation levels, regardless of the type of travel, incidences, and time. Specifically, extremely high temperatures (at 35 °C) increased SR during outbreaks by 12.5%-120% but shortened the time for mobility recovery. Increased rainfall (at 20 mm/day) added SRs by 12.5%-300%, with delayed effects reflected in cross-city movements. These compound impacts, with varying lagged responses, were aggravated in cities with high population density and low GDP levels. Our findings provide quantitative evidence to inform the design of preparedness and response strategies for enhancing urban resilience in the face of future pandemics and compound disasters.

1. Introduction

The ever-increasing worldwide environmental, socio-economic, and political crises may overlap in space and time, leading to the emergence of compound disasters (UNDRR, 2015). Unlike a single disaster and its cascading hazards, the interaction of multiple sourced disasters amplifies risks in broader societal and economic systems (Phillips et al., 2020; Walton et al., 2021; Sohn & Kotval-Karamchandani, 2023). The compounding COVID-19 pandemic and extreme weather events have already affected at least 139.2 million people and caused the death of

* Corresponding authors.
E-mail addresses: liuhaiyan@sml-zhuhai.cn (H. Liu), xuemei.bai@anu.edu.au (X. Bai), Shengjie.Lai@soton.ac.uk (S. Lai).
# These authors contributed equally to this work.

https://doi.org/10.1016/j.scs.2023.104872
Received 26 March 2023; Received in revised form 16 August 2023; Accepted 16 August 2023
Available online 18 August 2023

17,242 until August 2021 (Walton et al., 2021). Measures to combat the pandemic, including social distancing and travel restrictions, have impaired local governments' responses to weather hazards, thereby impacting urban life and livelihoods (Phillips et al., 2020; Walton et al., 2021). However, these restrictions are not choices off the table, especially for epidemics with high rates of transmission and severity (Lazarus et al., 2022). Moreover, as the global climate changes, there is an increased risk of extreme weather and cross-species viral transmission, suggesting that the co-occurrence of epidemics and extreme weather events may intensify in the future (Sobel & Tippett, 2018; Li & Zha, 2020; Kruczkiewicz et al., 2021; Carlson et al., 2022; Dodman et al., 2022; IPCC, 2022). Therefore, there is a critical need to understand the impacts of these compound disasters on urban life to facilitate future pandemic preparedness and urban resilience development (UNDRR, 2015; Zscheischler et al., 2018; Phillips et al., 2020).

The vulnerability of regions to compound disasters varies significantly due to their socioeconomic, demographic, cultural, environmental, and racial disparities (IPCC, 2012; Phillips et al., 2020). At different spatial and time scales, existing studies have demonstrated the devastating consequences of compound hazards (Zscheischler et al., 2018; Walton et al., 2021), the necessity of their impacts assessment (AghaKouchak et al., 2020; Stablein et al., 2022), and the importance of comprehensively considering compound factors in disaster prevention and mitigation (Vitolo et al., 2019; Matthews et al., 2019; van den Hurk et al., 2023). Descriptive and statistical analyses showed that poverty-stricken and marginalized areas are more affected by compound disasters and require a longer recovery time (Bai et al., 2020; Phillips et al., 2020; Walton et al., 2021; IPCC, 2022). However, there are gaps in understanding the quantitative impacts of compound disasters on human activities in cities, particularly in clarifying the differences between cities under varying conditions.

Human movement is one of the fundamental elements of human behaviour and socio-economic development, and its change can reflect people's adaptation to various contingencies (Lu et al., 2016; Hatchett et al., 2021; Hong et al., 2021; Yabe et al., 2022; Rajput et al., 2023). The mobility recovery process, bouncing back to the pre-disaster states, has been widely applied to measure the regional resilience characteristics (Stablein et al., 2022; Yabe et al., 2022; Liu et al., 2023). Researchers have developed proper metrics to evaluate (1) how disasters affect mobility patterns and to what extent, and (2) the duration of perturbations following crises (Zhang et al., 2019). While the urban recovery from COVID-19 outbreaks and extreme weather events has been investigated separately, their combined impact on the recovery of human mobility in cities has not been adequately quantified.

In this study, a data-driven dynamic mobility resilience analysis framework was designed to synthetically uncover the spatiotemporal heterogeneity of mobility recovery after compound disasters. The asynchronous travel restrictions of 313 Chinese prefecture-level cities under a zero-COVID policy in 2020–2022, together with extreme weather events, provided a real-world opportunity to investigate the impact of multiple crises for cities with different socio-economic settings. We built a spatiotemporal Bayesian hierarchical model, coupled with distributed lag non-linear models (DLNM) (Lowe et al., 2021), to untangle the delayed effects of COVID-19 incidence and intervention stringency on mobility recovery. The suppression risk (SR) metric, representing the relative effect of a factor that suppressed mobility recovery to the pre-pandemic level, was defined to measure the exposure-lag-response associations between different factors and the recovery of human mobility. We also assessed how the combined effects of the epidemic and extreme weather affected mobility, in terms of intensity and timing, by incorporating the interaction between the DLNM of incidence and extreme weather conditions into the model. Finally, how these compound disasters interactively affected travel within and between cities with different socioeconomic conditions were compared. The findings can help recognize the risks and vulnerabilities of cities in the face of compounding disasters, facilitating resource preparation and policy tailoring by governments and responses at local communities.

2. Related work

2.1. Mobility recovery after the COVID-19 outbreaks

The COVID-19 pandemic in 2020–2022 greatly impacted domestic and inter-region human mobility in complicated and unprecedented ways, notably through various travel restrictions as part of non-pharmaceutical interventions (NPIs) to mitigate virus transmission (Lai et al., 2020). Following the rollout of vaccines and the reduced severity of infections, governments have gradually relaxed local or regional travel restrictions, resulting in a rebound in local and regional mobility to pre-pandemic levels (Huang et al., 2021; Christidis et al., 2022). Recent studies have indicated that increases in outbreak size and intervention stringency were not linearly associated with decreases in mobility (Kim & Kwan, 2021; Christidis et al., 2022; Wu & Shimizu, 2022). Changes in travel patterns were generally observed days or even weeks after travel restrictions were enforced or eased (Tan et al., 2021; Mu et al., 2023). That is to say, the nonlinear and delayed effects of outbreaks and restrictions need to be considered in the mobility recovery after disasters.

During the pandemic, the intracity mobility and intercity movements were impacted by various factors and presented different recovery trajectories (Liu et al., 2021; Mu et al., 2023). Due to concerns about the risks of viral widespread across regions, long-distance transport and travel have been significantly reduced (Kellermann et al., 2022; Wang, et al., 2022). Thus, intercity travel was more affected in magnitude than intracity travel (Mu et al., 2023). Therefore, the recovery patterns of intra- and inter-city flows facing compound disasters should be separately evaluated to identify their differences.

2.2. Mobility recovery after extreme weather events

An extreme weather event is "rare as or rarer than the 10th or 90th percentile of a probability density function estimated from observations" (IPCC, 2022). It includes extreme heat event, extreme rainfall, hurricanes, tornadoes, and so on, which is supposed to be rare at a particular place and time of year. However, fixed thresholds of air temperatures and precipitation are commonly used for early warning of natural disasters like high temperatures, cold waves, and rainstorms in China (see *Supplementary-Extreme weather*). China also adopts these thresholds in official statistics of extreme weather (China Meteorological Administration, 2022). Therefore, this study used fixed thresholds to identify extreme weather events, while the spatial varying settings were used for sensitivity analysis of models and conclusions.

Previous research has shown that extreme temperature and rainfall could affect human mobility in terms of traffic volume, travel modes, and time spent on travel (Brum-Bastos et al., 2018; Kasmalkar et al., 2020; Wu et al., 2021; Mu et al., 2023), resulting in health and economic losses (UN Climate Change News, 2022). The US survey suggests cold, heat, and rainfall reduce outdoor movements (Obradovich & Fowler, 2017; Hatchett et al., 2021). Rainstorms perturb urban mobility in hours (Zhang et al., 2019). But traffic interruption caused by urban flooding, which is generated from rainstorms or hurricanes, might take days or weeks to recover (Kasmalkar et al., 2020; Hong et al., 2021; Rajput et al., 2023). Although Wu et al. (2021) proved weather-influenced mobility during the COVID-19 pandemic, the extent to which extreme weather events affect mobility recovery under disease outbreaks, in terms of intensity and timing, remains unclear.

2.3. Heterogeneity of mobility recovery after disasters

Travel recovery after disasters can also be affected by local socioeconomic, demographic, and geographic conditions, such as income (Li et al., 2021), population density (Liu et al., 2021; Kim & Kwan, 2021;

Mena et al., 2021), public holidays (Song et al., 2021; Ruktanonchai et al., 2021; Lai et al., 2022), and spillover effects of COVID-19 NPIs (Charoenwong et al., 2020; Zhao et al., 2021). For example, compared with the lockdown of a focal city, travel restrictions in neighbouring areas could lead to a larger decline of mobility (Zhao et al., 2021). This demonstrates the potential for policy and social spillover within an interconnected region in terms of human movement. These factors should all be considered to ascertain the spatiotemporal heterogeneity and mechanism of mobility variation in coupled crises.

Moreover, human mobility has a seasonal pattern (Lai et al., 2019; Lu et al., 2016; Song et al., 2021; Lai et al., 2022). Thus, using the average mobility data from weeks before the outbreaks as a pre-disaster baseline is unsuitable for long-term analysis. Seasonal variation derived from the mobility dataset before the pandemic could be used to adjust the mobility baseline.

3. Methods

3.1. Data collection and pre-processing

We obtained three publicly available city-level daily mobility datasets (i.e., intracity mobility intensity, inflow intensity, and outflow intensity) from Baidu's Qianxi (i.e. migration) data portal. Baidu anonymously collected mobility data of users through location-based services, when users opted in to share their locations. The data for over 1.2 billion monthly active mobile devices is gathered based on the global positioning system (GPS), IP address, location of signalling towers, and WIFI, for online searching, mapping, and a large variety of apps and software (Mu et al., 2023) The intracity mobility intensity was a relative percentage of the number of intracity movements compared to the number of residents in the city, while the inflow/outflow intensity was a relative magnitude of people inbound/outbound cities (Table 1). amongst the 368 administrative divisions with human mobility intensity given by Baidu, we selected daily mobility data for 313 cities in mainland China (Fig. 1, Supplementary) between 1 January 2021 and 30 December 2021 were collected to calculate the domestic mobility recovery degree of intracity and intercity (inflow/outflow) population movements in 2021, after the first wave of COVID-19 and the nationwide lockdown in the first half of 2020 in China. Rural prefectures (i.e., regions, leagues, and autonomous prefectures) were excluded because they did not have urban areas and urban socioeconomic information.

The mobility data from Baidu in two other periods, i.e., 1 October 2020 - 23 January 2021 and 1 January - 20 October 2022, were also collected for sensitive analysis. In addition, the data obtained from Baidu from January to March 2019 and 23 April 2013 - 29 April 2014 were used to identify the day-of-the-week fluctuations and weekly variants of mobility (Song et al., 2021). The impact of mobile device user growth to the baseline was also considered in the Supplementary.

The number of daily new COVID-19 cases in each city was collected from the official websites of the provincial and municipal health committees, spanning the period from 1 October 2020 to 20 October 2022. Not only laboratory-confirmed patients with symptoms but asymptomatic infections were counted since the authorities treated them similarly under China's zero-COVID policy (Liang et al., 2022). Then the transfer number of asymptomatic cases to confirmed ones who developed symptoms at a later stage was deducted from the number of daily new cases to avoid double counting. Daily incidence rate, i.e., the proportion of daily new cases reported in the total population of corresponding cities, was calculated to characterise the intensity of COVID-19 transmission in each city.

The policy stringency index obtained from the Oxford COVID-19 Government Response Tracker was used as the indicator of NPI implementation (Hale et al., 2021). It is a daily average strictness index of all eight containment and closure policies and public information campaigns. The index ranges from 0 to 100, with higher scores indicating stricter mobility restrictions. Given the national guidelines for implementing a zero-COVID policy and the lack of city-level NPI data in China, we used the provincial policy stringency index data to investigate the NPI effects on mobility recovery at the city level of each province.

Daily observed meteorological data, including mean temperature, maximum temperature, and total precipitation in 1990–2022, was downloaded from the Global Surface Summary of the Day dataset of NOAA's National Centers for Environmental Information (Data Identifiers: gov.noaa.ncdc:C00516). The inverse distance weighted interpolation method was applied amongst stations in China and its

Table 1
List of data used in this study.

Category	Data	Concept/explain	Source	Note
Mobility	Intracity mobility intensity	A relative percentage of the number of intracity movements compared to the number of residents in the city	Baidu's Qianxi data portal	Calculated as the recovery degree of intracity mobility
	Inflow/outflow intensity	A relative magnitude of people inbound/outbound cities	Baidu's Qianxi data portal	Calculated as the recovery degree of inflow/outflow
Epidemic-related	Number of daily new COVID-19 cases	The summary of laboratory-confirmed patients with symptoms and asymptomatic infections	Official websites of the provincial and municipal health committees	Calculated as the daily incidence rate
	Policy stringency index*	A daily average strictness index of all eight containment and closure policies and public information campaigns, indicating the stringency of policy implementation	Oxford COVID-19 Government Response Tracker (Hale et al., 2021)	
Weather	Daily observed meteorological data*	Daily mean temperature, maximum temperature, and total precipitation	NOAA's National Centers for Environmental Information	
	Weather variations*	Daily mean temperature and precipitation change between 2021 and the baseline calculation period		
	Weather anomalies*	Daily mean temperature and precipitation differences from their 30-year average from 1990 to 2019		
Spatial differentiation factors	Population size, urban density, total gross domestic product (GDP)*	Socioeconomic and demographic characteristics of cities	Statistical yearbooks of provinces and cities	
Temporal differentiation factors	Chunyun and public holidays *	The Spring Festival transport season holidays no less than three consecutive days	Official website of the General Office of the State Council of China	

* data directly introduced into modelling in this study.

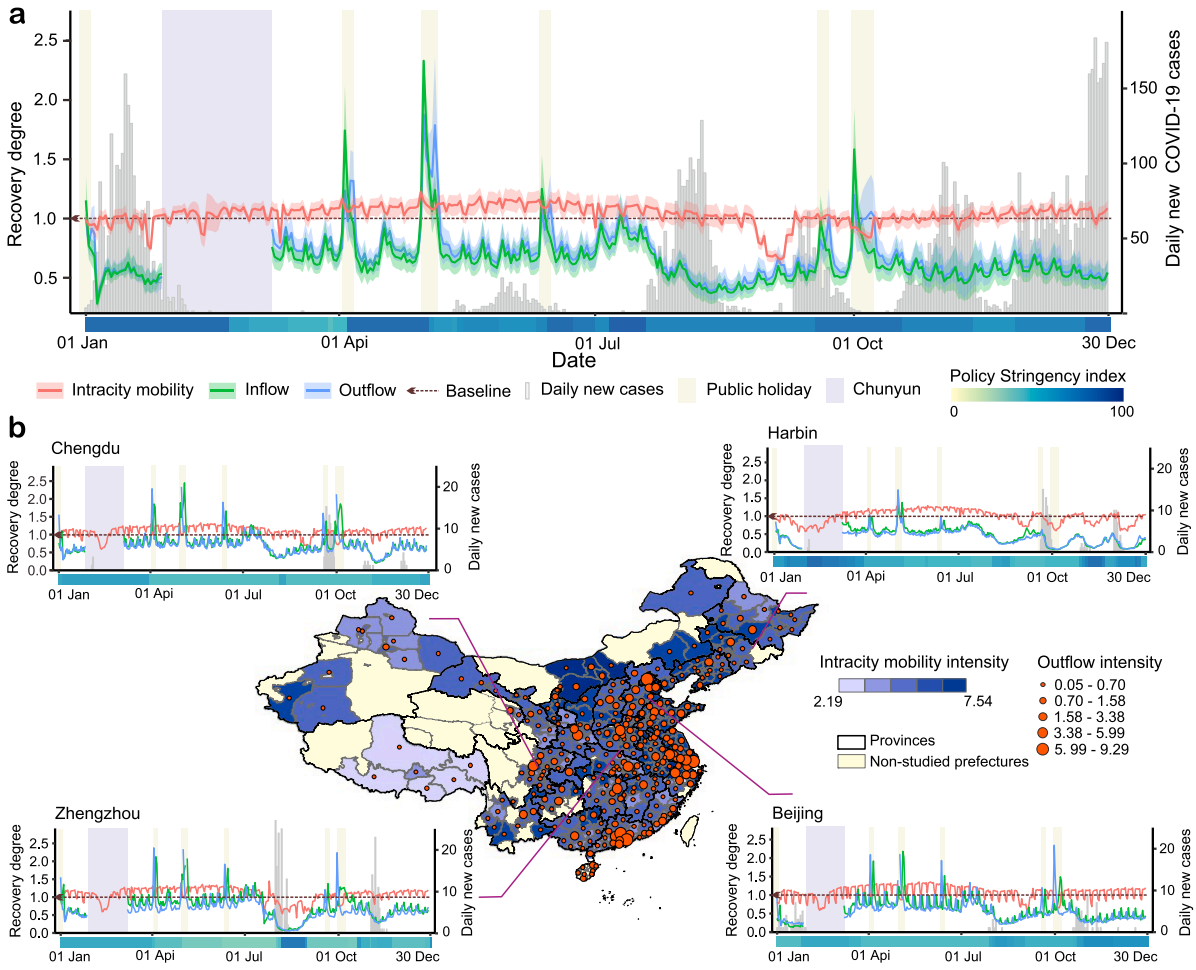

Fig. 1. Spatiotemporal heterogeneity of intra- and inter-city mobility recovery in 313 Chinese cities in 2021.
a, Changes of intracity mobility, outflow, and inflow in 2021. The recovery degrees of inflow/outflow are not presented for the *Chunyun* period and its following week (i.e., 28 January -14 March 2021). Daily new COVID-19 cases include laboratory-confirmed cases and asymptomatic infections reported by the 313 studied cities. **b**, Spatiotemporal heterogeneity in recovery trajectories between cities. The map shows the geographical locations of cities and their pre-pandemic relative intracity mobility and outflow intensity on 16 January 2019, provided by the Baidu location-based service. Both intensities were classed into five levels by the Natural Break method in ArcGIS 10.6. The changes in mobility across space and time are demonstrated by taking the daily recovery trajectories of four cities, i.e., Chengdu, Harbin, Zhengzhou, and Beijing, in 2021.

surrounding countries in 0.1-degree spatial resolution to obtain the spatial average of daily temperature and precipitation for each city (Khouni et al., 2021). This geoprocessing model was created with ModelBuilder of ArcGIS 10.6 software (Supplementary Fig. S1). The model was looped 12,053 times (days) to get the daily temperature and precipitation datasets for 313 Chinese cities in 33 years. For the three days (i.e., 11–13 February 2021) with limited observation data, re-analysed temperature data from ERA-5 (Hersbach et al., 2022) and gridded daily precipitation data from China National Climate Centre, both in 0.1-degree spatial resolution, were used instead (Supplementary Fig. S2). To distinguish whether the weather or weather change affected the mobility recovery, weather variations and weather anomalies were brought into analysis (Table 1). Additionally, the data of population size, urban density, and total gross domestic product (GDP) for cities at the end of 2019 were obtained to stratified cities under pre-pandemic socioeconomic and demographic characteristics. Both data came from the statistical yearbooks of provinces and cities. Besides, the periods of *Chunyun* and public holidays over the years were obtained from the official website of the General Office of the State Council of China. R programming language (version 4.1.3) was used to implement data processing and geospatial analysis.

3.2. *Measuring the recovery degrees of mobility*

A three-step methodology was developed to quantify the intracity and intercity mobility recovery patterns and degrees across cities, comparing to pre-pandemic baselines. Seasonality of mobility was taken into account by using a weekly variation coefficient derived from a longer pre-pandemic mobility dataset from 2013 to 2014 (Song et al., 2021). The degree of mobility recovery during the pandemic was defined as the percentage of human movement compared with the baseline.

Step 1: Identifying the pre-pandemic baseline based on the temporal change patterns of mobility. To understand the seasonal fluctuations and day-out-of-week periodicity over time, we visualised the magnitude and change trajectories of different types of travels in the datasets of January-March 2019 and April 2013 - April 2014. Since the intracity mobility was relatively stable on a weekly scale (Supplementary Fig. S3-S4), we used each city's daily average of intracity mobility intensity from 2 January to 22 January 2020, the continuous three week before the Wuhan lockdown, as the baseline of pre-pandemic movements within each city. Since the inflow and outflow presented significant changes between weeks, hinting at seasonal variations (Supplementary Fig. S3-S4), weekly variation coefficients were considered for their

baseline calculation.

Step 2: Identifying the pre-pandemic inflow/outflow baseline based on their weekly variation coefficients. Weekly variations were extracted from the intercity mobility datasets for 2013–2014. We used the daily average inflow/outflow intensity of city i during the week before *Chunyun* in 2014 (i.e., 09–15 January 2014) - denoted as $I14_i$- as the baseline for evaluating seasonal changes in mobility. For data available from1 January to 29 April 2014, the weekly variation coefficients of city i on week w (where w<18) were expressed as: $V_{i,w} = \frac{I14_{i,w}}{I14_i}$, where $I14_{i,w}$ is the daily average inflow/outflow intensity of city i on week w of 2014. For date from 30 April (where $w \geq 18$), the intercity mobility data from 2013 was used: $V_{i,w} = \frac{I13_{i,w}+Ic_i}{I14_i}$, where $I13_{i,w}$ is the daily average intensity of city i on week w of 2013. Ic_i is the annual inflow/outflow change for city i, calculated by comparing the daily average mobility intensity during the overlapping week of 2013 and 2014 (i.e., 23–29 April). Each city's inflow/outflow baseline was the average daily intensity for the week prior to the *Chunyun* period in 2020 (i.e., 3–9 January) (I_i) multiplied by the weekly variation coefficients: $I_{i,w} = I_i \times V_{i,w}$. The inflow/outflow baseline quantified the intercity mobility in 2020 before the COVID-19 pandemic, serving as a basis for comparison with following mobility patterns.

Step 3: Measuring the degrees of mobility recovery. The magnitude of city-level daily mobility recovery in 2021 was measured by the proportion of daily mobility intensity in 2021 to that on the same day of the Gregorian calendar in 2020. The formulas are $R^I_{i,t} = \frac{I_{i,t}}{I_{i,w}}$, $R^{IN}_{i,t} = \frac{IN_{i,t}}{IN_{i,w}}$, and $R^{OUT}_{i,t} = \frac{OUT_{i,t}}{OUT_{i,w}}$, where $I_{i,t}$, $IN_{i,t}$, and $OUT_{i,t}$ are the intracity mobility, inflow, and outflow intensity of city i on day t, respectively. $I_{i,w}$, $IN_{i,w}$, and $OUT_{i,w}$ are the intracity, inflow, and outflow baseline of city i on the week w of day t, respectively. As this study focused on the usual mobility beyond major holiday periods, considering the misalignment of the Spring Festival (i.e. Lunar New Year) holiday between lunar and Gregorian calendars, the period of major Chinese New Year's seasonal migration (also known as *Chunyun* period) and one week after (from 28 January to 15 March 2021) was excluded from the intercity mobility recovery modelling.

3.3. Quantifying non-linear and delayed effects of factors on mobility recovery

We built spatiotemporal Bayesian hierarchical models for the recovery degrees of intracity mobility, inflow, and outflow, respectively, across 313 Chinese cities from 1 January to 30 December 2021. It was assumed that the recovery degrees conform to Gaussian distributions$R_{i,t}|\mu_{i,t},\sigma \sim \mathrm{N}(\mu_{i,t},\sigma^2)$, where $\mu_{i,t}$ was the corresponding distribution expectation (or mean) and σ was its standard deviation. The Poisson and negative binomial distribution baseline models were also tested but failed to get enough initial value to explain residual overdispersion to spatiotemporal random effects (See below). Integrated nested Laplace approximations in a Bayesian framework were used to estimate model parameters in R version 4.1.3 (Rue et al., 2009).

A base model was constructed for mobility recovery, comprising two spatiotemporal random effects, holiday, and socioeconomic factors. The first spatiotemporal effect accounted for the day-of-the-week periodicity of mobility by a cyclic random walk model of order one (RW1), which allowed the mobility recovery in one day to depend on its immediate preceding day (Lowe et al., 2021). The other spatiotemporal random effect accounted for the inter-week variability in cities by a modified Besag-York-Mollie (BYM) model (Riebler, et al., 2016). It included an unstructured spatial random effect to explain city-specific noise (e.g. health care, testing ability, and policy adherence disparities) and a conditional autoregressive model to account for geographical and social spillover effects (Petherick et al., 2021; Lai et al., 2022). For both random effects, we applied the Penalized Complexity (PC) prior for the precision with Pr=0.01(Simpson et al., 2017). Besides, the holiday and GDP factors were included in the base model as fixed effects to eliminate the impact of short public holidays and socioeconomic levels on mobility. The base model was as follows:

$$R_{i,t} = \alpha + \beta_{c(i/p)d(i)} + U_{c(i)w(t)} + S_{c(i)} + Vh + Vg_i$$

where α is an intercept, $\beta_{c(i/p)d(i)}$ is the city- or provincial- level day-of-the-week random effects (see Supplementary *Spatiotemporal effects*), $U_{c(i)w(i)}$ is the week-specific unstructured spatial random effect at the city level, $S_{c(i)}$ is the structured spillover effects at the city level, Vh is the fixed effect for public holidays, and Vg_i is the fixed effect for city-level socioeconomic status.

Distributed lag nonlinear models (DLNMs) were included to access the exposure-lag response associations between the SR of motilities and epidemics (Gasparrini, 2014). The delayed effects of outbreaks and interventions were assessed by 14 days and up to 28 days when necessary, with natural cubic splines selected for both the exposure and the lag dimensions. The epidemic model was:

$R_{i,t} = \alpha + \beta_{c(i/p)d(i)} + U_{c(i)w(t)} + S_{c(i)} + Vh + Vg_i + f.l(In,d)_i + f.l(Psi,d)_i$ where $f.l(In,d)_i$ is the incidence DLNM and $f.l(Psi,d)_i$ is the policy stringency DLNM (Supplementary *Distributed lag nonlinear models*). The "dlnm" package in R version 4.1.3 was used for analysis.

Assuming exposure to the epidemics would reduce travel, we used the suppression risk (SR) to describe the relative risk of mobility reduced to below the pre-pandemic baseline in the situation of variables relative to the normal case. $SR = 1 - \frac{P(R|E)}{P(R|\neg E)}$, where $P(R|E)$ is the posterior ratio of the exposure and $P(\neg E)$ is the prior ratio of exposure. The values of SR close to 0 indicate the exposure might not result in mobility change from the pre-pandemic baseline and the increase of SR suggests increased risks by the exposure. Given the scarcity of research samples at higher incidences, which may reduce the generalisability of model output made their output interpretation cannot represent the general situation, we estimated the maximum SR of mobility under all incidences to analyse the most impact of local outbreaks on mobility resilience. Meanwhile, travels were assumed to be affected during one outbreak. The delayed effects of a low incidence (i.e., the average minimum incidence in five cities with the smallest population size) near the end of outbreaks were explored to estimate how long the repercussions might last after outbreaks ebb. Since the resurgence of infections was likely to rebound the SR, only the time before SR reaches its lowest value or 0 was considered as the delayed effect of outbreaks on mobility recovery.

To assess the mobility adaptation under compound disasters, we calculated the linear interactions between incidence DLNM and extreme weather by changing the centring weather conditions before introducing them into the Bayesian hierarchical model. The performance of weather factors, weather variations, and weather anomalies were compared to find out which factors could better explain the mobility change. The selected temperature and precipitation variables were centred at different levels (see Supplementary *Methods*), according to the indicators of cold waves, hot waves, and rainstorms in the meteorological disaster early warning signal system implemented by the China Meteorological Administration. The interacted cross-basis variables and the weather variable as a fixed effect were added to the epidemic model to build incidence-weather models (formulas in Supplementary Table S4-S5). Further, to access the response of cities with different socioeconomic settings, the linear interaction between the compound disasters and urban density/GDP levels was tested (specific interaction levels and formulas see Supplementary).

The goodness-of-fit criteria, measured by the deviance information criterion (DIC) and the log score (Lowe et al., 2021), were applied to compare model performances and identify the best-fitting model for intracity mobility, inflow, and outflow recoveries, respectively. DIC balances model accuracy against complexity by estimating the number of effective parameters, while the log scores measure the predictive power of the model when excluding one data point at a time. For both

measures, smaller values denote better-fitting models. The association between DLNMs and SRs of mobility in better-fitting models were used to interpret the results in coordination.

3.4. Sensitivity and validation

To check the robustness of models and results, we also conducted sensitivity analyses from five perspectives. First, the maximum SR under fixed incidences interacted with extreme weather was checked in each model in 2021 to identify whether the result was stable across the different scales of outbreaks. Second, the maximum SRs under compound risks for each types of travel at two different times were compared, i.e., from 1 October 2020 to 23 January 2021 and from 1 January to 30 December 2021, to identify weather the result was robust across time. Third, the interacted levels were changed to verify the results. In comparing the impact of compound risks in cities with different GDP levels, the maximum SR not only under the same incidence but the same number of reported infections were evaluated and compared. Since the log-transformed incidence (*In*) and GDP (Vg) was significantly correlated in cities with outbreaks (r=-0.54, P<-0.001), the linear regression model: $In = 9.78 - 0.68 \times Vg$ was applied to calculate the incidences across GDP levels. Fourth, settings for extreme weather events, extreme high/low temperatures specifically, were changed to confirm the robustness of conclusions. On the one hand, we have modified the settings for high and low temperatures in the sensitivity analysis, which used winter data from October 2020 to January 2021 and did not have extremely high temperatures over 35 °C (see Supplementary *Sensitivity analysis*). On the other hand, spatial varying extremes at the city level, i.e., 10th/90th percentiles of daily maximum temperature in the past 30 years from 1990 to 2019, were introduced to consider regional differences. Fifth, the models with one DLNM and with the combination of two DLNMs were compared to determine whether the increase of DLNMs would affect the results of included DLNM, i.e., whether the SR of incidence might be affected by un-included factors.

To further validate the improvement of more complex, data-driven mobility recovery models, the difference in mean absolute error (MAE) were calculated between the base models and the selected models to identify the proportion and location of cities for which improved model fit. A cross-validation analysis was conducted based on the parameters and hyperparameters of the best-fitting model by leaving out one week each time. The posterior predictive distributions of the mobility recoveries were estimated by extracting 1000 random values from a Gaussian distribution with mean and standard deviation estimated from the model for the excluded week prediction. We fitted 52 times for the intracity mobility model and 46 times for the intercity one. The posterior predictive distributions of mobility recoveries for each week (i.e., mean and 95% credible interval) were grouped at the provincial level and compared with the observed ones.

4. Results

4.1. Spatiotemporal heterogeneity of mobility in recovery trajectories

To identify the trajectory of mobility recovery, we defined the degree of relative mobility at 100% or higher implying a return to the pre-pandemic level. Fig. 1 shows that intracity and intercity travel for Chinese cities held distinct recovery trajectories, corresponding to local outbreaks and restrictions. In general, intracity mobility rebounded more than intercity travel (Fig. 1a). The degree of recovery averaged at 103.5% (Interquartile [IQR]: 96.0%, 110.2%) in 2021 for intracity mobility, followed by 64.6% (IQR: 56.7%, 76.1%) for inflow, and 69.4% (IQR: 56.7%, 81.7%) for outflow. In 282 days (77.5%) of the year 2021, average intracity mobility was higher than that in 2020. For most of the year – 317 days (95.5%) for inflow and 281 days (84.6%) for outflow – intercity mobility did not return to pre-pandemic levels. The temporal changes in incoming and outgoing travel were similar, with a Pearson correlation of 0.91 (P<0.001) between their degrees of recovery. Notably, all the dates where inflow and outflow recovered by more than 105% were either short public holidays (3–7 days long) or one day preceding and following them (Fig. 1a).

Recovery of mobility also depended on the scale of outbreaks. Under the zero-COVID policy, 103 out of the 313 studied Chinese cities confirmed 7455 locally infected people between 1 January and 30 December 2021, with a maximum of 176 daily new cases at the city level. Coincident with new infections, the degree of mobility recovery decreased to 82.5%, 46.9%, and 45.8% of the total average for intracity travel, inflow, and outflow, respectively, while the level of recovery across cities was negatively correlated with the incidence of COVID-19 (i.e., r=-0.51, P<0.001 for intracity mobility, r=-0.48, P<0.001 for inflow, and r=-0.49, P<0.001 for outflow, respectively). However, even if the local transmission was fully interrupted, mobility in affected cities could not resume immediately. Examples of this were observed in Chengdu and Harbin in November 2021, and in Zhengzhou and Beijing in August (Fig. 1b), suggesting that epidemics might have delayed mobility recovery. In addition, policy stringency, temperature, and precipitation were also correlated with the degree of mobility recovery (P<0.01) (see Supplementary Table S1-S3).

4.2. Nonlinear and delayed impacts of the epidemic on mobility recoveries

The comparison of goodness-of-fit criteria, shown in Supplementary Table S4-S5, indicated the introduction of DLNM improved model adequacy statistics compared with incidence or policy factor with no lags, proving the rationality and necessity of considering the delayed effects in understanding mobility recovery after epidemics (see *Methods*). Including incidence as DLNM resulted in the best-fitting intracity model, while the combination of incidence and policy stringency resulted in the best-fitting intercity models (hereafter referred to as epidemic models). The provincial interventions barely explained the intracity mobility recovery discrepancy at the city level in 2021 but affected cross-city movements.

Outputs from the epidemic models showed that the higher COVID-19 incidence and stricter policies were associated with the greatest SR amongst the three different types of travel, with varying lags (Fig. 2). The greatest SR of intracity mobility was found on the day that the highest number of cases was reported in each outbreak (maximum SR 0.08, 95% confidence interval (CI): 0.07–0.09), followed by a decrease in SR over time (Fig. 2a). The SR under a low incidence scenario increased at a lag of 0–21 days, suggesting that population movement within cities might still be affected within three weeks after an outbreak. The maximum SR of inflow was found at the highest incidence lagged by 3 days (0.05, 95% CI: 0.03–0.10) (Fig. 2b), while that of outflow (0.06, 95% CI: 0.03–0.14) happened with no time lag (Fig. 2c). The SR under outbreaks of inflow and outflow increased at a lag of 0–6 days. In addition, the strictest policies were also most likely to suppress intercity mobility. The maximum SR reached 0.17 (95% CI: 0.15–0.19) for inflow (Fig. 2e) and 0.18 (95% CI: 0.17–0.20) (Fig. 2f) for outflow on the day implementing the strictest policy, and then decreased over time. The SR of inflow and outflow increased after the exposure to interventions at a lag of 0–4 days (Fig. 2e and 2f).

4.3. Combined effects of epidemics and extreme weathers on mobility recovery

To distinguish the effects of weather, its variation, and anomalies on mobility recovery under the pandemic, weather-related factors were added to the epidemic model as fixed effects and compared their model goodness-of-fit (see Supplementary Table S4-S5). The results show that the inclusion of daily maximum temperature had the most significant model-fit improvements for all three types of travel, compared to average temperature, temperature variation from the baseline period, and temperature anomaly (i.e., the difference from the 30-year average

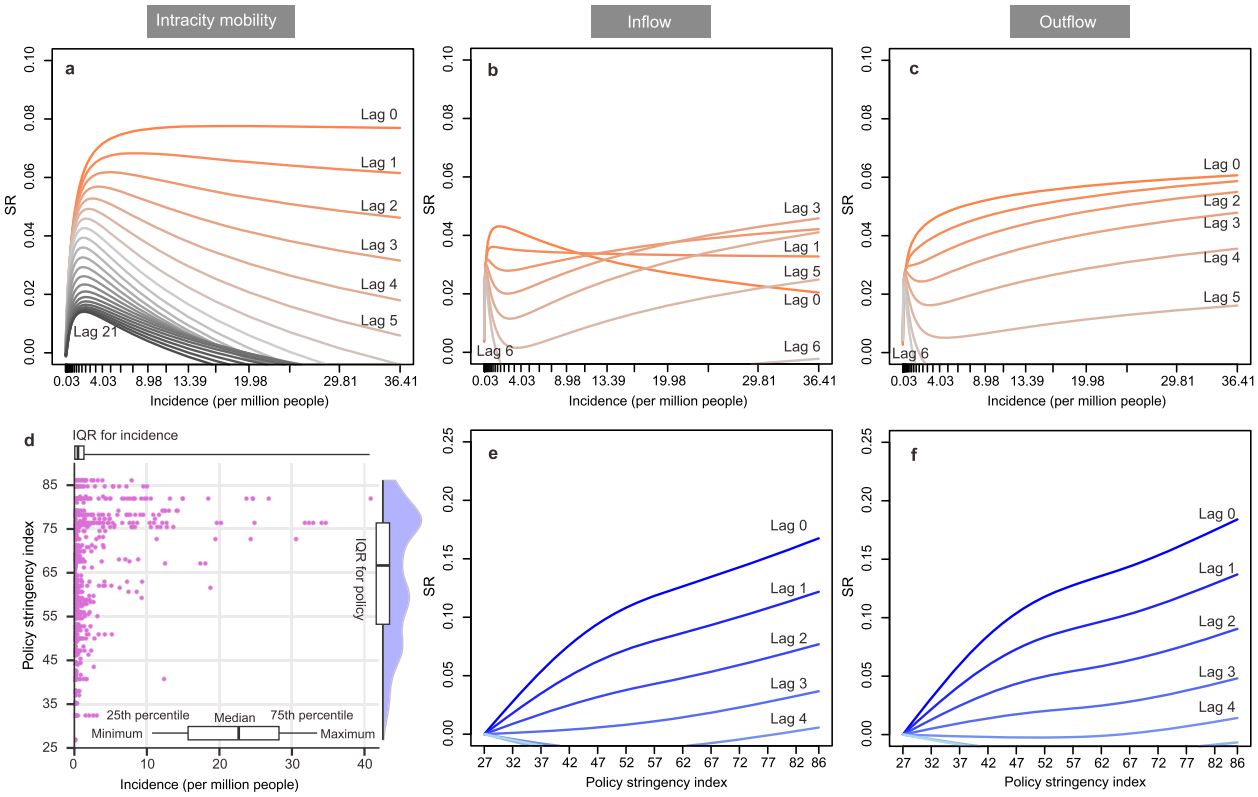

Fig. 2. Mobility recovery in lagged responses to varying scenarios of COVID-19 incidence and intervention policy stringency.
a, b, and c The suppression risks (SRs) of mobility after the report of COVID-19 incidences (i.e., daily new cases per million people in each city) at different time lags, compared with no new case condition. **d,** The data distribution (points) and probability density (boxplot) of incidence and policy stringency index under outbreaks. **e and f,** The SRs of inflow and outflow under the policy implementation with different stringencies, respectively, compared with the loosest interventions of an index at 27.

from 1990 to 2019). Meanwhile, precipitation anomaly also improved the model fit for all three types of travel (detailed in Supplementary), which was used for the following interaction analysis.

We added the interaction between incidence and extreme daily maximum temperatures/precipitation anomaly to the epidemic model to identify how extreme weather affected mobility recovery after the pandemic, in terms of intensity and timing. As illustrated in Fig. 3, the maximum SR always occurred under the interaction of incidence and high temperature/high abnormal precipitation, regardless of travel type. Compared with extremely low temperature (4 °C), extremely high temperature (35 °C) uplifted the maximum SR after outbreaks for intracity mobility from 0.08 (95% CI: 0.07–0.10) to 0.09 (95% CI: 0.06–0.12), for inflow from 0.03 (95% CI: 0.02–0.10) to 0.11 (95% CI: 0.05–0.19), and for outflow from 0.05 (95% CI: 0.02–0.13) to 0.10 (95%

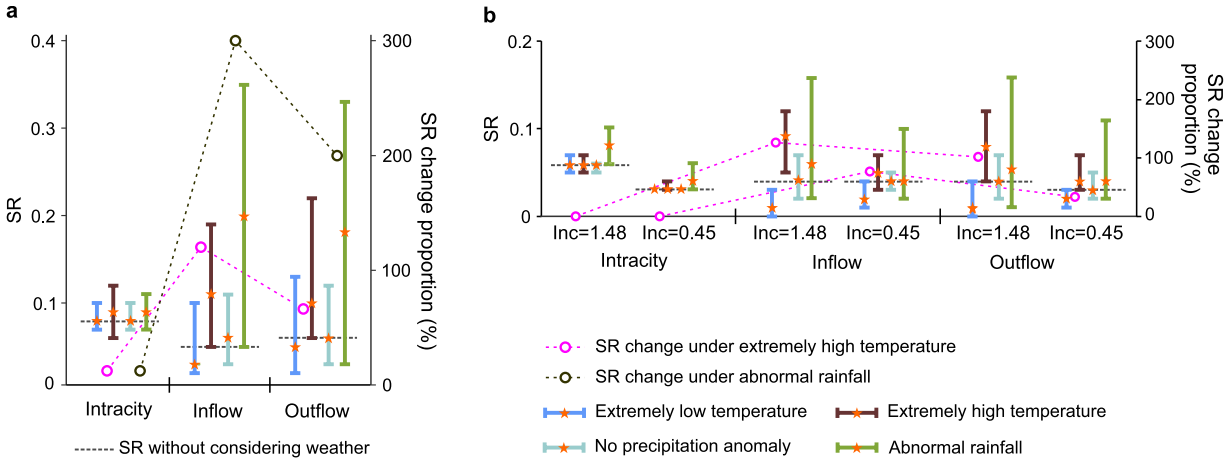

Fig. 3. Suppression risks of mobility under epidemics and different temperature and precipitation anomaly levels.
a, The maximum SR of intracity travel, inflow, and outflow under COVID-19 outbreaks in 2021, interacted with extremely low temperature (4 °C), extremely high temperature (35 °C), no precipitation anomaly (precipitation anomaly as 0 mm/d) and abnormal rainfall (20 mm/d), relative to no COVID-19 case situation. **b,** The maximum SR of intracity, inflow, and outflow under fixed incidences, i.e., 1.4 cases per million people (around the 75th percentile of all incidences) and 0.45 cases per million people (around the median), interacted with temperature and precipitation anomaly in 2021. The secondary y-axis represents the proportion of changes in maximum SR under extreme weather relative to SR without considering weather conditions.

CI: 0.06–0.22) (Fig. 3a). The interaction with extreme heat, rather than cold, heightened the SR of mobility after epidemics. Compared with normal precipitation conditions, the high rainfall (20 mm/d) increased the maximum SR from 0.08 (95% CI: 0.07–0.10) to 0.09 (95% CI: 0.07–0.11) for intracity mobility, from 0.06 (95% CI: 0.03–0.11) to 0.20 (95% CI: 0.05–0.35) for inflow, and from 0.06 (95% CI: 0.03–0.12) to 0.18 (95% CI: 0.03–0.33) for outflow (Fig. 3a). This conclusion remained the same under different incidence rates (Fig. 3b). Moreover, by changing fixed threshold values of extreme weather or adopting rare temperatures at the city level (Supplementary-Sensitivity analysis), the sensitive analyses proved the robustness of the result (Supplementary Fig. S5).

Compared with the intracity mobility, intercity movement was more sensitive to the extreme weather under the pandemic (Fig. 3). Compared with outputs from the epidemic model, extremely high temperature aggravated the maximum SR after outbreaks by 12.5% for intracity mobility, 120% for inflow, and 66.7% for outflow (Fig. 3a). Compared with no consideration of rainfall, rainstorms increased the maximum SR after outbreaks by 12.5% for intracity mobility, 300% for inflow, and 200% for outflow. The impact of abnormal precipitation on human movements under epidemics was greater than that of high temperatures. Under the same incidence, the results still held. The SR for intracity mobility remained stable across temperatures but increased by 33.3% under increased rainfall (20 mm/d) relative to without considering weather conditions (Fig. 3b).

To estimate how long the repercussions might last after outbreaks ebb, we explored the delayed effect of a low incidence (i.e., the average minimum incidence in five cities with the smallest population size) near the end of outbreaks. Fig. 4 shows high temperature shortened the lag effect of outbreaks, while the delayed recovery of mobility after abnormal heavy rain was mainly reflected in cross-city movements. Extremely high temperature (35 °C) shortened the lag effect of epidemics by 6 days (i.e., from 21 days to 15 days) for intracity mobility and by less than 1 day for intercity mobility (Fig. 4a). In contrast, intra- and inter- city movements responded differently to the combination of epidemics and rainstorms. The increased rainfall shortened the lag effects of outbreaks, i.e., from 21 days to 16 days under 20 mm/d and to 19 days under 50 mm/d. Meanwhile, the lag times of inflow and outflow recoveries after outbreaks were extended from 0 to 7 days to 2–11 days after the abnormal increase of precipitation by 50 mm/d (Fig. 4b). The delayed effects of high temperatures on the mobility recovery after outbreaks were consistent with the findings above, although at different lag times, no matter in the analysis of different times (Supplementary Fig. S6) or in analysis adopting spatiotemporal various extremes (Supplementary Fig. S7).

4.4. *Differentiation of effects across socio-economic conditions*

We found that the inclusion of urban population density and GDP both improved the model fit for all three types of travel (see Supplementary Table S4-S5), suggesting that the socio-economics of cities might affect local mobility recovery following the simultaneous occurrence of extremely high temperatures and outbreaks. The higher the urban population density, the greater the impact of combined disasters on mobility but the quicker the mobility recovery (Table 2 and Fig. 5a). The maximum SR of intracity mobility under all incidences increased from 0.08 (95% CI: 0.06–0.10) in sparse cities with 3000 people/km^2 to 0.10 (95% CI: 0.08–0.12) in dense cities with 8000 people/km^2, relative to no cases (Table 1). The increment was from 0.04 (95% CI: 0.03–0.10) to 0.05 (95% CI: 0.02–0.13) for inflow and from 0.05 (95% CI:

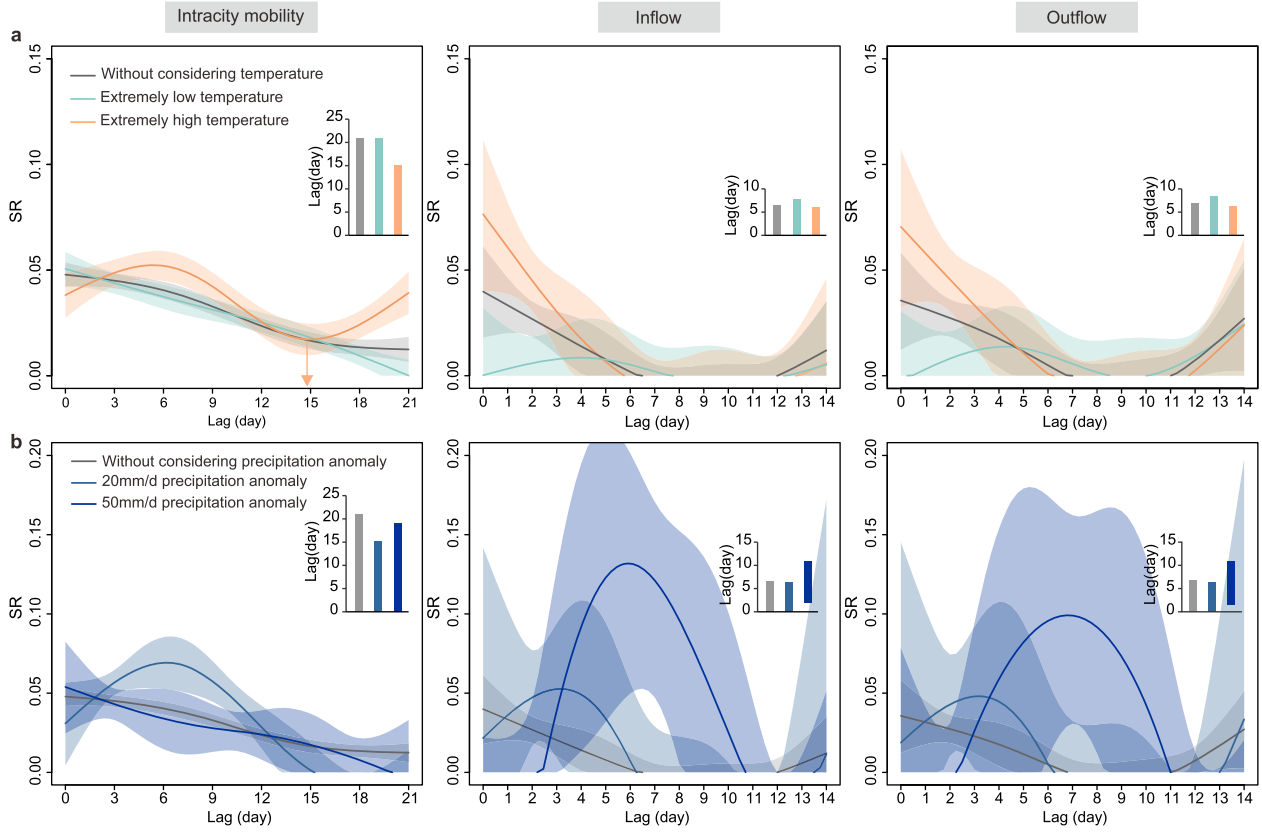

Fig. 4. Lag-response of mobility under the interaction of COVID-19 outbreaks and extreme weather conditions.
a, High temperature shortened the lag effects of outbreaks. **b,** The delayed recovery of mobility after abnormally heavy rain was mainly reflected in cross-city movements. The lag time under outbreaks was interpreted from the average minimum incidences in five cities with the smallest population size, i.e., 1.1 daily new cases per million people, suggesting the aftershock of outbreaks on mobility.

Table 2
Maximum SR of mobility recovery under the collision of outbreaks and extremely high temperature (35 °C), by urban population density and GDP levels.

Socioeconomic conditions		Intracity mobility	Inflow	Outflow
Urban density	Sparse City	0.08 (0.06–0.10)	0.04 (0.03–0.10)	0.05 (0.03–0.11)
	Medium-density City	0.09 (0.07–0.11)	0.05 (0.03–0.11)	0.05 (0.03–0.10)
	Dense City	0.10 (0.08–0.12)	0.05 (0.02–0.13)	0.06 (0.03–0.12)
GDP	Low GDP	0.09 (0.08–0.11)	0.08 (0.05–0.11)	0.09 (0.06–0.13)
	Medium GDP	0.10 (0.08–0.12)	0.06 (0.03–0.09)	0.07 (0.04–0.12)
	High GDP	0.15 (0.12–0.18)	0.08 (0.03–0.13)	0.08 (0.04–0.14)

Note: The maximum SR and its 95% CI under different scenarios, relative to no COVID-19 case situation, are presented in the table. Details are provided in the Supplementary *Methods*.

0.03–0.11) to 0.06 (95% CI: 0.03–0.12) for outflow (Table 2). Under the same incidence, the increasing impact of combined disasters on mobility also existed (Fig. 5a). Compared with sparsely populated cities, the lag effects of overlapping outbreaks and heatwaves in dense cities were slightly lower (Fig. 5a). In addition, although the maximum SRs for intracity mobility and inflow were found in wealthy cities (Table 1), all three types of movement were most likely to be suppressed in cities with lower GDP levels, and mobility in wealthier cities took longer to recover amidst a combination of epidemics and extreme heat (Fig. 5b).

Under extremely high temperatures, cities with different socio-economic attributes exhibited more noticeable variations in their recovery following the epidemic. When compared to sparsely populated cities, densely populated cities experienced an increase of 0% to 25% in maximum SR under compound disasters and 0% to 16.7% under outbreaks (Fig. 6a). Similarly, compared to cities with lower GDP levels, wealthier cities witnessed increments of maximum SRs, ranging from 40% to 75% under combined impacts, and from 33.3% to 50% under outbreaks (Fig. 6b). These comparisons were made while considering the same low incidence rate.

The sensitivity and validation analyses revealed that the intensity and changes of SRs, under the interaction of outbreaks and high temperatures across different socio-demographic settings, appeared coherent across different periods in 2020–2021 (Supplementary Table S6 and Fig. S8). The impact of COVID-19 incidence on changes in intracity mobility was relatively stable, regardless of policy impact (Supplementary Table S7 and Fig. S9). Compared with the base model, the incidence-temperature-density models reduced the mean absolute errors in 169 (54.0%) of all 313 cities for intracity travel, 313 (100%) for inflow, and 296 (94.6%) for outflow, suggesting improved model fits in these cities (locations can be found in Supplementary Fig. S10). In addition, the out-of-week posterior predictive mean estimates of

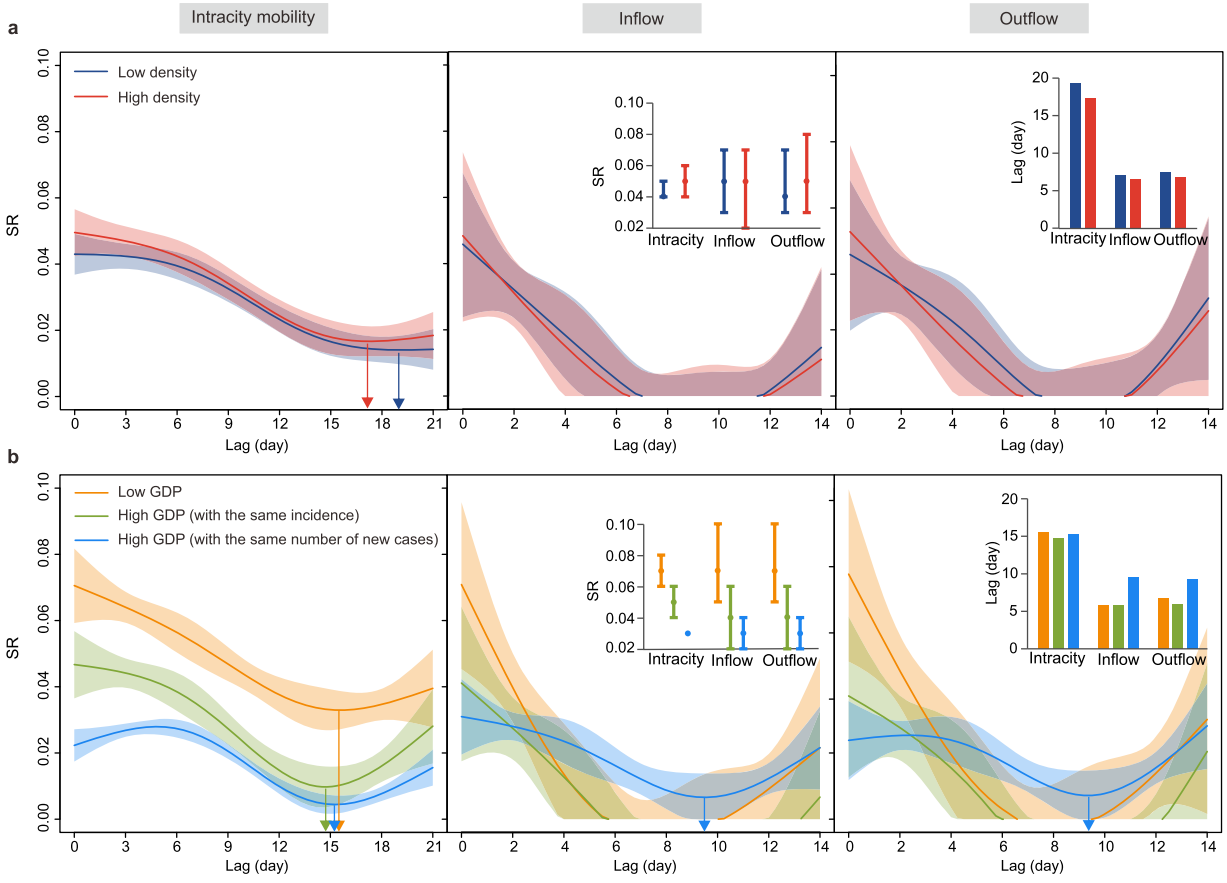

Fig. 5. Lag-response of mobility under outbreaks and extremely high temperatures in cities with different population density and GDP levels.
a, The lag-response of intracity, inflow, and outflow under the compound COVID-19 outbreaks and extremely high temperature (daily maximum temperature=35 °C) disasters in sparse cities (dark blue, urban density=3000 people/km^2) and dense cities (red line, urban density=8000 people/km^2) at the average of the minimum incidence in five cities with the smallest population size (1.1 cases per million people), relative to no new case conditions. **b,** The lag-response of intracity, inflow, and outflow under the compound outbreaks and extremely high temperature disasters in cities with low GDP (orange line, lower quartile of GDP=87.5 billion RMB) and high GDP (green line, upper quartile of GDP=312.8 billion RMB) at the same incidence (1.1 cases per million people), or at the same number of daily new cases (see *Methods*, blue line for cities with high GDP at the incidence of 0.45 cases per million people), relative to no new case conditions. Shaded areas represent 95% CI.

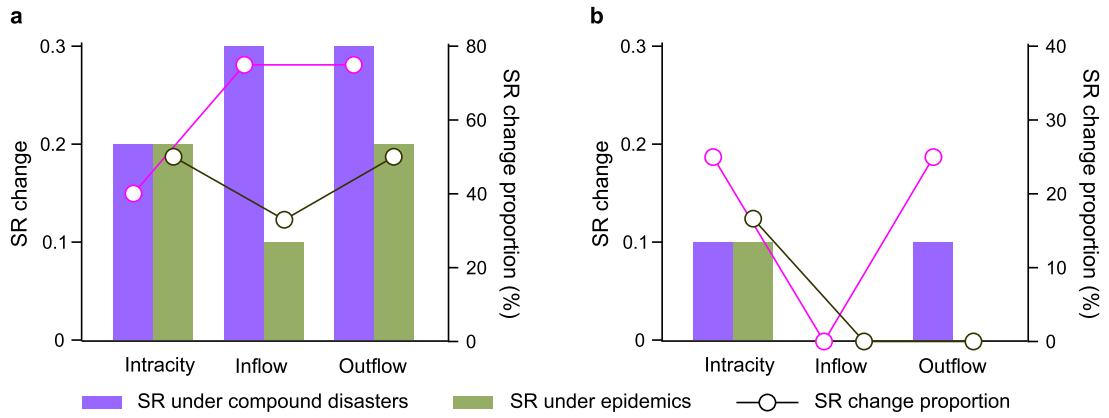

Fig. 6. Comparison of SRs under compound disasters and epidemics in cities with different socio-economic conditions.
a, The changes of the maximum SRs in low-GDP cities, compared with those in high-GDP cities. **b,** The changes of the maximum SRs in dense cities compared with those in sparse cities. All comparisons were made while considering the same low incidence rate (1.1 cases per million people).

recovery degrees suggested our model successfully distinguished mobility recoveries between provinces, with better fitting curves for intercity mobility than intracity (Supplementary Fig. S11-S13).

5. Discussion

This study used spatiotemporal Bayesian inference models to investigate the non-linear and delayed effects of epidemics on intra- and intercity mobility recoveries across 313 Chinese cities under extreme weather events and different socioeconomic conditions during the pandemic in this research. It allowed the interaction of disasters, not only human-induced epidemics but also natural hazards, providing methodology and framework for the impact assessment of the multiple crises. By quantifying the combined effects of epidemics and extreme weather, this study enriches the existing knowledge of urban recovery after compound disasters.

This study found that intracity movements were less vulnerable to extreme weather than intercity ones under the pandemic. Facing epidemics and extreme weather events, citizens might reduce unnecessary cross-city travel, but intracity movements related to commuting and maintaining daily life would be preserved (Kellermann et al., 2022; Wang, et al., 2022). For example, following the extreme rainfall in Zhengzhou in July 2021, the government first resumed public transport operation to ensure the intracity movements of people (Tencent News, 2021). Delays in urban recovery caused by the interaction of outbreaks and heavy rainfall were mainly reflected in cross-city movements. Thus, the resilience of intercity and intracity movements needs to be considered separately in preparation for compound disasters.

Gravity models have widely been used to estimate human movement and explore its push-pull factors (Zipf, 1946). Assumptions of such models are that human movement between regions is inversely proportional to the distance between them but positively related to a range of demographic and socioeconomic factors such as total population, urbanisation and income (Garcia et al., 2015; Sorichetta et al., 2016; Lai et al., 2019). However, this research shows that patterns contrary to those predicted by gravity models might have occurred during the recovery of population movements during the compound disasters. The greater suppression risk of inflow under outbreaks appeared in cities with higher GDP/density/population size levels, which would be considered destinations of population immigration in gravity models. Travel-related NPIs prevent people from entering big cities to reduce the risk of infection exposure or epidemic spread, which might be one of the reasons for the delayed mobility recovery in wealthier cities.

The high-density and low-GDP cities would be the most vulnerable ones confronting compound disasters. In 2021, the log-transformed GDP level for cities with outbreaks was significantly negatively correlated with their policy stringency index (r=-0.65, P<0.001). Cities with lower GDP adopt stricter policies than cities with higher GDP/population size to prevent local virus transmission since their local health care conditions, economical safety nets, and transport supply were inadequate to handle large-scale outbreaks (Charoenwong et al., 2020; Mena et al., 2021; Wang, et al., 2022). However, it should be noted that these cities were already highly vulnerable to extreme weather events (IPCC, 2022). In order to enhance anticipatory adaptation in disaster preparation, it is important for the government to strike a balance between public safety and climate adaptation measures, avoiding the amplification and application of one-size-fits-all restrictions. Furthermore, additional financial support should be allocated to these vulnerable cities to enhance their basic infrastructure and social protection systems, thereby building resilience to future climate shocks. It is crucial to recognize that these efforts require long-term planning and implementation. Therefore, preventive actions should be prioritized and taken seriously by all stakeholders.

The study is also subject to several limitations. First, we examined mobility changes under a zero-COVID policy in China, which has been lifted. However, extreme weather still challenges the epidemic response of cities, like the temporal overlapping of the rainy season and cholera outbreaks in 2022 across Southern Africa. The research provides a practical analytical framework for analysing urban response and resilience after combined disasters, whose findings and implications could inform integrated strategies for pandemic preparedness and climate adaptation. Second, a provincial-level policy stringency index was applied, instead of the city-level policy stringency index, due to the data accessibility. The policy stringency in China could vary across cities and even communities due to the varying epidemic situations and official response, leading to a reduced generalisability of provincial policies. Even though we proved that the inclusion of policy stringency did not influence the model results of incidence, it was established on the limited usage of stay-at-home orders from October 2020 to December 2021. The mobility response to the epidemic in 2022 in China was also explored, when different cities adopted the strictest travel restrictions to curb the community transmission of the highly contagious Omicron variant, thus affecting the interpretation of extreme weather on mobility recovery (Supplementary *Results*). Introducing city-level policies might better explain the urban mobility adaption processes, which would be improved in future studies. Third, the pre-pandemic baseline of intercity mobility in 2020 was adjusted by the seasonality from 2013 to 2014, bringing the mobility change caused by extreme weather conditions in 2013–2014 into the baseline calculation. Such inclusion was almost inevitable in the data-driven analysis. Weather variations between 2021 and the baseline calculation period were included to rule out the assumption that weather variations dominated mobility changes. Last

but not least, we solely considered the interaction of epidemics and daily maximum temperature/precipitation anomalies, whereas meteorological factors may be superimposed to trigger more significant threats. For example, precipitation at extremely low temperatures might result in freezing conditions, delaying movement recovery. The effects of combined meteorological factors need to be explored in further research.

6. Conclusion

This study revealed the intracity and intercity (including inflow and outflow) mobility recovery processes at the city level and day scale under the compound disasters of the pandemic and extreme weather events, through long-term and large-scale quantitative research. The findings indicated that extreme weather, i.e., extremely high temperatures and extremely high levels of precipitation anomalies, aggravated the suppression risk of mobility after epidemics, which was further intensified in high-density or low-GDP cities. Heat shortened the lag effects of outbreaks on mobility recovery, while abnormal rainfall delayed intercity mobility recoveries during outbreaks. Given the combined risks of natural disasters under climate change and the potential for future epidemics caused by other emerging infectious diseases, the findings and data-driven analytical framework from this study can serve as methodological and transferable knowledge to support urban resilience quantification under multiple crises. Future research on the combined effects of epidemics and extreme weather should be strengthened in the climate change environment.

Data and code availability

The mobility data were collected from Baidu's Qianxi data portal (https://qianxi.baidu.com/#/), which is not publicly available due to licensing agreements. The processed degrees of mobility recovery and other relevant data are available at: https://github.com/fionaliuhy/Compound-Disaster/tree/main/Data. Code used in this paper is available in the following GitHub repository: https://github.com/fionaliuhy/Compound-Disaster. Ethical clearance for collecting and using secondary data in this study was granted by the institutional review board of the University of Southampton (No. 61,865). All data were supplied and analysed in an anonymous format, without access to personal identifying information.

Declaration of Competing Interest

The authors declare that they have no known competing financial interests or personal relationships that could have appeared to influence the work reported in this paper.

Data availability

All the data and code have been updated based on the comments and shared in "Data and code availability" section.

Acknowledgements

We thank the researchers and organisations who generated and publicly shared the mobility, epidemiological, intervention, and analysing code used in this research. This study was supported by the National Institute for Health (MIDAS Mobility R01AI160780), the Bill & Melinda Gates Foundation (INV-024911), the National Nature Science Foundation of China (72025405, 91846301, 72088101), and the Southern Marine Science and Engineering Guangdong Laboratory (Zhuhai) (SML2021SP102). The funders of the study had no role in study design, data collection, data analysis, data interpretation, or writing of the report. The corresponding authors had full access to all the data in the study and had final responsibility for the decision to submit for publication. The views expressed in this article are those of the authors and do not represent any official policy.

Supplementary materials

Supplementary material associated with this article can be found, in the online version, at doi:10.1016/j.scs.2023.104872.

References

AghaKouchak, A., et al. (2020). Climate extremes and compound hazards in a warming world. *Annual Review of Earth and Planetary Sciences, 48*, 519–548.

Bai, X., Nagendra, H., Shi, P., & Liu, H. (2020). Cities: Build networks and share plans to emerge stronger from COVID-19. *Nature, 584*, 517–520.

Brum-Bastos, V. S., Long, J. A., & Demšar, U. (2018). Weather effects on human mobility: A study using multi-channel sequence analysis. *Computers, Environment and Urban Systems, 71*, 131–152.

Carlson, C. J., Albery, G. F., Merow, C., et al. (2022). Climate change increases cross-species viral transmission risk. *Nature, 607*, 555–562.

Charoenwong, B., Kwan, A., & Pursiainen, V. (2020). Social connections with COVID-19 affected areas increase compliance with mobility restrictions. *Science Advances, 6*, eabc3054.

China Meteorological Administration (2022). China climate bulletin. (accessed 30 April 2022); http://www.cma.gov.cn/zfxxgk/gknr/qxbg/202203/t20220308_4568477.html.

Christidis, P., Ciuffo, B., & Vespe, M. (2022). Regional mobility during the Covid-19 pandemic: Analysis of trends and repercussions using mobile phones data across the EU. *Case Studies on Transport Policy, 10*, 257–268.

Dodman, D.B. et al. (2022). Cities, Settlements and Key Infrastructure. In: Climate change 2022: Impacts, adaptation and vulnerability (pp. 907–1040).

Garcia, A. J., Pindolia, D. K., Lopiano, K. K., & Tatem, A. J. (2015). Modeling internal migration flows in sub-Saharan Africa using census microdata. *Migration Studies, 3*, 89–110.

Gasparrini, A. (2014). Modeling exposure–lag–response associations with distributed lag non-linear models. *Statistics in Medicine, 33*, 881–899.

Hale, T., Angrist, N., Goldszmidt, R., et al. (2021). A global panel database of pandemic policies (Oxford COVID-19 Government Response Tracker). *Nature Human Behaviour, 5*, 529–538.

Hatchett, B. J., et al. (2021). Mobility data to aid assessment of human responses to extreme environmental conditions. *Lancet Planetary Health, 5*, e665–e667.

Hersbach, H., Bell, B., Berrisford, P., Biavati, G., Horányi, A., Muñoz Sabater, J., Nicolas, J., Peubey, C., Radu, R., Rozum, I., Schepers, D., Simmons, A., Soci, C., Dee, D., & Thépaut, J-N. (2022). ERA5 hourly data on single levels from 1940 to present. *Copernicus Climate Change Service (C3S) Climate Data Store (CDS)*. https://doi.org/10.24381/cds.adbb2d47 (Accessed on 30 October 2022).

Hong, B., Bonczak, B. J., Gupta, A., & Kontokosta, C. E. (2021). Measuring inequality in community resilience to natural disasters using large-scale mobility data. *Nature Communications, 12*, 1870.

Huang, B., et al. (2021). Integrated vaccination and physical distancing interventions to prevent future COVID-19 waves in Chinese cities. *Nature Human Behaviour, 5*, 695–705.

IPCC. (2012). *Managing the risks of extreme events and disasters to advance climate change adaptation. a special report of working groups I and II of the intergovernmental panel on climate change [Field, C.B., V. Barros, T.F. Stocker, D. Qin, D.J. Dokken, K.L. Ebi, M.D. Mastrandrea, K.J. Mach, G.-K. Plattner, S.K. Allen, M. Tignor, and P.M. Midgley (eds.)]* (p. 582). Cambridge, United KingdomNew York, NY, USA: Cambridge University Press.

IPCC. (2022). *Climate change 2022: Impacts, adaptation, and vulnerability. contribution of working group ii to the sixth assessment report of the intergovernmental panel on climate change [H.-O. Pörtner, D.C. Roberts, M. Tignor, E.S. Poloczanska, K. Mintenbeck, A. Alegría, M. Craig, S. Langsdorf, S. Löschke, V. Möller, A. Okem, B. Rama (eds.)]* (p. 3056). Cambridge, UKNew York, NY, USA: Cambridge University Press. Cambridge University Press. https://doi.org/10.1017/9781009325844. pp.

Kasmalkar, I. G., et al. (2020). When floods hit the road: Resilience to flood-related traffic disruption in the San Francisco Bay Area and beyond. *Science Advances, 6*, eaba2423.

Kellermann, R., Conde, D. S., Robler, D., Kliewer, N., & Dienel, H-L (2022). Mobility in pandemic times: Exploring changes and long-term effects of COVID-19 on urban mobility behavior. *Transportation Research Interdisciplinary Perspectives, 15*, Article 100668.

Khouni, I., Louhichi, J., & Ghrabi, A. (2021). Use of GIS based inverse distance weighted interpolation to assess surface water quality: Case of Wadi El Bey, Tunisia. *Environmental Technology & Innovation, 24*, Article 101892.

Kim, J., & Kwan, M.-P. (2021). The impact of the COVID-19 pandemic on people's mobility: A longitudinal study of the U.S. from March to September of 2020. *Journal of Transport Geography, 93*, Article 103039.

Kruczkiewicz, A., et al. (2021). Opinion: Compound risks and complex emergencies require new approaches to preparedness. *Proceedings of the National Academy of Sciences of the United States of America, 118*, Article e2106795118.

Lai, S., et al. (2019). Exploring the use of mobile phone data for national migration statistics. *Palgrave Communications, 5*, 34.

Lai, S., et al. (2020). Effect of non-pharmaceutical interventions to contain COVID-19 in China. *Nature, 585*, 410–413.

Lai, S., et al. (2022). Global holiday datasets for understanding seasonal human mobility and population dynamics. *Scientific Data, 9*, 17.
Lazarus, J. V., et al. (2022). A multinational Delphi consensus to end the COVID-19 public health threat. *Nature, 611*, 332–345.
Li, L., & Zha, Y. (2020). Population exposure to extreme heat in China: Frequency, intensity, duration and temporal trends. *Sustainable Cities and Society, 60*, Article 102282.
Li, Y., et al. (2021). Vulnerability evaluation of rainstorm disaster based on ESA conceptual framework: A case study of Liaoning province, China. *Sustainable Cities and Society, 64*, Article 102540.
Liang, W., et al. (2022). The dynamic COVID-zero strategy on prevention and control of COVID-19 in China. *National Medical Journal of China, 102*(4), 239–242.
Liu, Y., et al. (2021). Associations between changes in population mobility in response to the COVID-19 pandemic and socioeconomic factors at the city level in China and country level worldwide: A retrospective, observational study. *Lancet Digital Health, 3*, e349–e359.
Liu, Y., et al. (2023). Quantifying human mobility resilience to the COVID-19 pandemic: A case study of Beijing, China. *Sustainable Cities and Society, 89*, Article 104314.
Lowe, R., et al. (2021). Combined effects of hydrometeorological hazards and urbanisation on dengue risk in Brazil: A spatiotemporal modelling study. *Lancet Planetary Health, 5*, e209–e219.
Lu, X., et al. (2016). Unveiling hidden migration and mobility patterns in climate stressed regions: A longitudinal study of six million anonymous mobile phone users in Bangladesh. *Global Environmental Change, 38*, 1–7.
Matthews, T., Wilby, R. L., & Murphy, C. (2019). An emerging tropical cyclone–deadly heat compound hazard. *Nature Climate Change, 9*, 602–606.
Mena, G. E., et al. (2021). Socioeconomic status determines COVID-19 incidence and related mortality in Santiago, Chile. *Science (New York, N.Y.), 372*, abg5298.
Mu, X., et al. (2023). Structural changes in human mobility under the zero-COVID strategy in China. *Environment and Planning B: Urban Analytics and City Science, 0*, 1–16.
Obradovich, N., & Fowler, J. H. (2017). Climate change may alter human physical activity patterns. *Nature Human Behaviour, 1*, 0097.
Petherick, A., et al. (2021). A worldwide assessment of changes in adherence to COVID-19 protective behaviours and hypothesized pandemic fatigue. *Nature Human Behaviour, 5*, 1145–1160.
Phillips, C. A., et al. (2020). Compound climate risks in the COVID-19 pandemic. *Nature Climate Change, 10*, 586–588.
Rajput, A. A., Nayak, S., Dong, S., & Mostafavi, A. (2023). Anatomy of perturbed traffic networks during urban flooding. *Sustainable Cities and Society*, Article 104693.
Riebler, A., Sørbye, S. H., Simpson, D., & Rue, H. (2016). An intuitive Bayesian spatial model for disease mapping that accounts for scaling. *Statistical Methods in Medical Research, 25*(4), 1145–1165.
Rue, H., Martino, S., & Chopin, N. (2009). Approximate Bayesian inference for latent Gaussian models by using integrated nested Laplace approximations. *Journal of the royal statistical society: Series b (statistical methodology), 71*, 319–392.
Ruktanonchai, C. W., Lai, S., Utazi, C. E., et al. (2021). Practical geospatial and sociodemographic predictors of human mobility. *Scientific Reports, 11*, 15389.
Simpson, D., Rue, H., Riebler, A., Martins, T. G., & Sørbye, S. H. (2017). Penalising model component complexity: A principled, practical approach to constructing priors. *Statistical Science, 1-28*, 28.
Sobel, A.H. & Tippett, M.K. (2018). Chapter 1 - Extreme Events: Trends and Risk Assessment Methodologies. In Z. Zommers, & K. Alverson (Eds.), Resilience (pp. 3–12).
Sohn, W., & Kotval-Karamchandani, Z. (2023). Risk perception of compound emergencies: A household survey on flood evacuation and sheltering behavior during the COVID-19 pandemic. *Sustainable Cities and Society*, Article 104553.
Song, B., et al. (2021). Human mobility models reveal the underlying mechanism of seasonal movements across China. *International Journal of Modern Physics C, 33*, Article 2250054.
Sorichetta, A., et al. (2016). Mapping internal connectivity through human migration in malaria endemic countries. *Scientific Data, 3*, Article 160066.
Stablein, M. J., et al. (2022). Compounding disasters in Puerto Rico: Pathways for virtual transdisciplinary collaboration to enhance community resilience. *Global Environmental Change, 76*, Article 102558.
Tan, S., et al. (2021). Mobility in China, 2020: A tale of four phases. *National Science Review, 8*, nwab148.
Tencent News (2021). Heave rain caused multiple roads and air traffic to be interrupted in Zhengzhou, and the urban traffic is gradually resuming. (accessed 20 August 2021); https://new.qq.com/rain/a/20210721A0E9WA00.
UN Climate Change News (2022). Climate Change Leads to More Extreme Weather, but Early Warnings Save Lives. (accessed 30 April 2022); https://unfccc.int/news/climate-change-leads-to-more-extreme-weather-but-early-warnings-save-lives.
UNDRR (United Nations Office for Disaster Risk Reduction) (2015). Sendai Framework for Disaster Risk Reduction 2015-2030. (accessed 16 June 2022); http://www.unisdr.org/we/inform/publications/43291.
van den Hurk, B., et al. (2023). Consideration of compound drivers and impacts in the disaster risk reduction cycle. *iScience, 26*, Article 106030.
Vitolo, C., Di Napoli, C., Di Giuseppe, F., Cloke, H. L., & Pappenberger, F. (2019). Mapping combined wildfire and heat stress hazards to improve evidence-based decision making. *Environment International, 127*, 21–34.
Walton, D., Arrighi, J., van Aalst, M., & Claudet, M. (2021). *The compound impact of extreme weather events and COVID-19. An update of the number of people affected and a look at the humanitarian implications in selected contexts* (p. 34). Geneva: IFRC.
Wang, J., Huang, J., Yang, H., & Levinson, D. (2022). Resilience and recovery of public transport use during COVID-19. *NPJ Urban Sustainability, 2*, 18.
Wu, L., & Shimizu, T. (2022). Analysis of the impact of non-compulsory measures on human mobility in Japan during the COVID-19 pandemic. *Cities (London, England), 127*, Article 103751.
Wu, Y., Mooring, T. A., & Linz, M. (2021). Policy and weather influences on mobility during the early US COVID-19 pandemic. *Proceedings of the National Academy of Sciences, 118*, Article e2018185118.
Yabe, T., Rao, P. S. C., Ukkusuri, S. V., & Cutter, S. L. (2022). Toward data-driven, dynamical complex systems approaches to disaster resilience. *Proceedings of the National Academy of Sciences, 119*, Article e2111997119.
Zhang, F., Li, Z., Li, N., & Fang, D. (2019). Assessment of urban human mobility perturbation under extreme weather events: A case study in Nanjing, China. *Sustainable Cities and Society, 50*, Article 101671.
Zhao, M., Holtz, D., & Aral, S. (2021). Interdependent program evaluation: Geographic and social spillovers in COVID-19 closures and re-openings in the United States. *Science Advances, 7*, eabe7733.
Zipf, G. K. (1946). The P_1 P_2/D hypothesis: On the intercity movement of persons. *American Sociological Review, 11*, 677–686.
Zscheischler, J., et al. (2018). Future climate risk from compound events. *Nature Climate Change, 8*, 469–477.